

THE SPECTRAL CONTENT OF THE TORQUE LOADS ON A TURBINE GEAR TOOTH¹

Herbert J. Sutherland

Wind Energy Technology
Sandia National Laboratories
Albuquerque, NM 87185-0708

and

Daniel P. Burwinkle

NMERI
University of New Mexico
Albuquerque, NM 87106

ABSTRACT ¹

The torque loads on two classes of wind turbine gearboxes are analyzed using a time-at-torque technique and a rainflow counting technique to determine the cyclic loads on the gear teeth. The two techniques are compared and contrasted to one another using representative samples of the time histograms from a Micon 65 and the Sandia/DOE Test Bed wind turbines. To place these differences in perspective, Miner's Rule is used to determine the damage produced by each of the distributions. The damage analyses illustrate that the differences in the distributions are minimal.

INTRODUCTION

The typical design technique used for a gearbox is based on the maximum torque transmitted through the box and by the spectral content (time varying portion) of the load. The spectral content is usually characterized by a "service factor." Recommended service factors for normal applications are supplied by gearbox manufactures and standardized by the American Gear Manufacturers Association (AGMA). As an example, a service factor of 1.0 is recommended for relatively short duration applications involving uniform loads, as with cooling fans or rotary pumps for liquids, and a factor of 2.0 is recommended for continuous applications involving reciprocating loads, as with cooling tower fans or beet slicers in the sugar industry. The unique torque spectrum for a wind

turbine precludes its characterization by any of the standard categories.

In a technique that is better suited for the characterization and analysis of the loads on a typical wind turbine gearbox, McNiff, Musial, and Errichello (1990) developed a "time-at-level" histogram for the loads on the gearbox. In this technique, the torque applied to the gearbox is characterized by the total time the gearbox will be subjected to a given magnitude of torque. The development of these loads is based on a point-by-point "binning" of the time series data by magnitude, see Akins (1990). The service lifetime analysis assumes that each torque bin is applied to the gearbox in a quasi-static manner; namely, the torque is a slowly varying function of time.² The service lifetime of the gearbox is then determined using a Miner's Rule analysis that meets AGMA standards. The time-at-level technique is best characterized as a macro-approach to the analysis.

From a materials standpoint, the macro-approach may be overlooking some important loads on the gearbox. To determine if important fatigue loads are being overlooked, a rain-flow cycle counting technique is used to determine the cyclic loads on an "average tooth" in a wind turbine gearbox. The rainflow technique is best characterized as a micro-approach to the analysis.

The time histograms from two classes of wind turbine gearboxes are analyzed here to compare and contrast the macro and the micro techniques for characterizing the cyclic loads on

¹This work is supported by the U.S. Department of Energy under contract DE-AC04-94AL85000.

²A "slowly varying function of time" implies that the torque loads on the gear teeth produce a single stress cycle per each tooth engagement.

their gearboxes. The first gearbox is on a Micon 65, which was studied previously by McNiff, Musial, and Errichello (1990), and the second is on the Sandia/DOE Test Bed.

DESIGN GUIDE FOR GEARBOXES

The AGMA Standard (1976) for the design of spur and helical gears uses the “relatively simple, linear, cumulative fatigue damage criteria proposed by Miner (Miner’s Rule) ... to ascertain the effects of variable loading on the life of the gearing.” In this procedure, the “duty cycle” (transmitted torque) is related to the stress in an average tooth through a series of standard formulas that are based on the geometry of the gears. The damage³ is then calculated using Miner’s Rule (Osgood, 1982) and the S-N gear characterization specified by the standard. A typical S-N diagram used by AGMA for alloy steels case carburized to Rc 58-63 case hardness and Rc 30-42 core hardness is shown in Figure 1. If no “fatigue” or “endurance” limit is assumed for this material at the 2E6 cycle break (see Figure 1), the slope of the S-N curve below the break is equivalent to a 34.5 MPa (5 ksi) drop from 2E6 to 1E8 cycles.

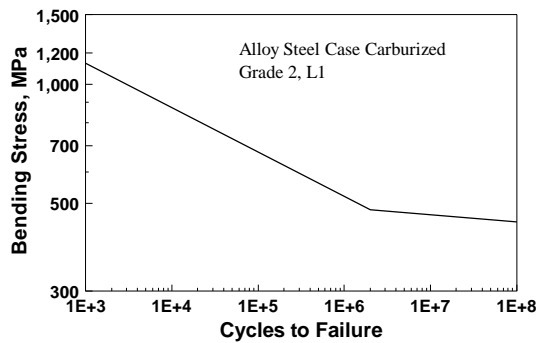


Figure 1. Typical S-N Diagram for Carbonized Steel Gears.

Other S-N diagrams are available in the literature and directly from gear manufacturers as proprietary data. For this analysis, we will use the data cited in Figure 1 exclusively.

THE TURBINES

Data from two turbines are analyzed in this paper. One is the Micon 65, and the other is the Sandia/DOE Test Bed. The former is a horizontal axis wind turbine (HAWT) and the latter is a vertical axis wind turbine (VAWT).

Micon 65

As reported by McNiff, Musial, and Errichello (1990), the Micon 65 kW turbine is a three-bladed, Danish-designed wind turbine. The 7.5 meter blades were made from fiber reinforced

polyester resins and equipped with pitching tips for centrifugal over speed control. The blades connect to a ridged, fixed pitch hub which rotates at a synchronous speed of 48 rpm. Peak power from the rotor is regulated by aerodynamic stall, which is designed to flatten the power curve near 65 kW in high winds. The low-speed shaft (LSS) enters a two-stage, parallel-shaft, helical gearbox with an output speed of about 1200 rpm. Typical time series data for the LSS torque are shown in Figure 2.

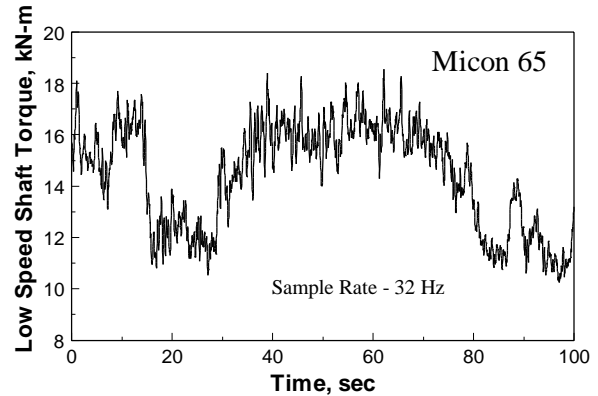


Figure 2. Typical Time Series Data for the Low Speed Shaft Torque on the Micon 65.

The gearbox of this turbine was analyzed previously by McNiff, Musial, and Errichello (1990). They showed that the premature failures of the gearbox were the result of the very high stresses created by the high-speed shaft brake. Based on a Miner’s Rule analysis, they predicted that the gear life could be increased by a factor of 25 if the standard high-speed brake were replaced with a dynamic brake or modified with a damper.

Sandia 34-m Test Bed

The Test Bed is a 34-meter diameter VAWT erected by Sandia National Laboratories near Bushland, Texas (just west of Amarillo) for research purposes. The turbine and site are equipped with a large array of sensors that permit the characterization of the turbine under field conditions.⁴ In this report, we examine gear fatigue during operation of the turbine at a constant 28 rpm. The gearbox is a multi-stage helical gearbox that increases the LSS speed by a factor of 47.56 (to approximately 1330 rpm). The gearbox also turns the transmitted torque through a right angle [the LSS is a vertical shaft and the high-speed shaft is a horizontal shaft]. Typical series data for the LSS torque are shown in Figure 3.

³The damage is the fractional part of the service lifetime consumed by the stress cycles under analysis.

⁴Veers (1990) put together a compendium of the technical papers written on this turbine.

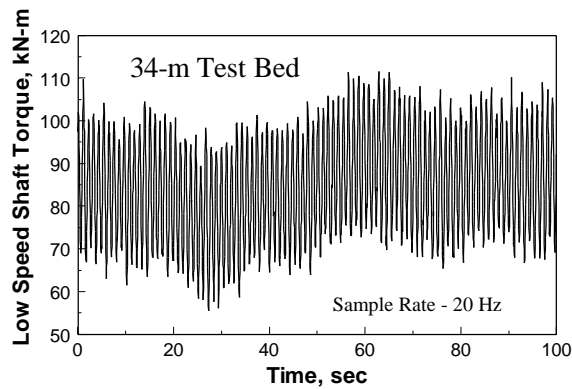


Figure 3. Typical Time Series Data for the Low-Speed Shaft Torque on the Test Bed.

CYCLIC LOADS

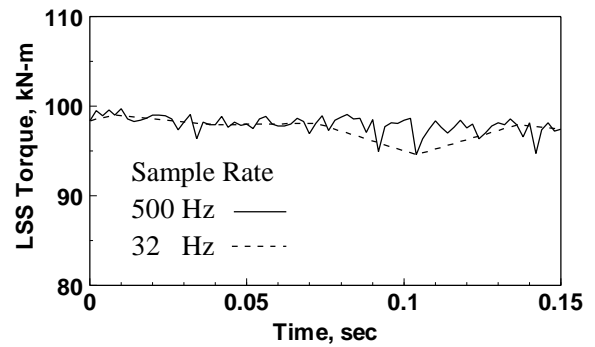
The analysis of the stresses on the gear teeth within a helical gearbox is the subject of a very large body of literature. The AGMA Standard (1976) and Information Sheet (1989) describe a consensus technique for converting shaft torque to the stress in a gear tooth. We will not go into this technique here. Suffice it to say, that the technique provides a linear multiplier for the torque to convert it to tooth stress. For this paper, we will report torque because that is the variable usually reported when sizing gearboxes.

Data Analysis

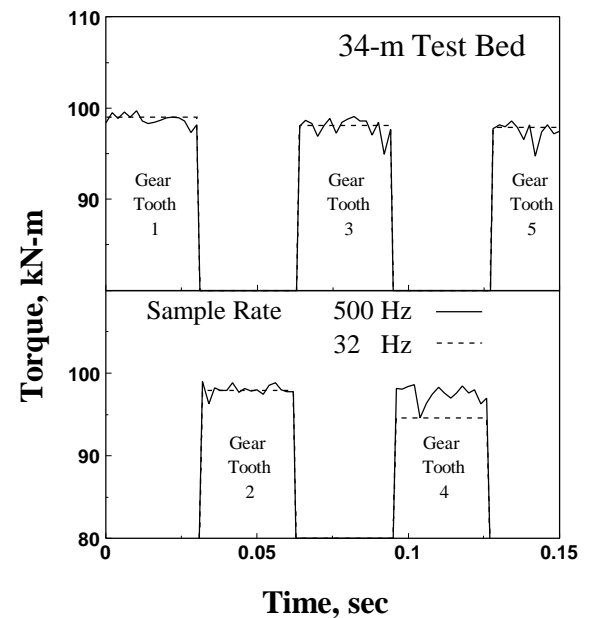
The LSS torque time series data for the Test Bed, equivalent to the data shown in Figure 3, are shown with an expanded time scale in Figure 4a. Each tooth on the pinion gear “samples” a different section of this torque history. As depicted simplistically in Figure 4b, each tooth is engaged for approximately 0.03 seconds. During engagement, the tooth is transmitting torque. Before and after each engagement, the tooth is unloaded.

Two time series are shown in Figure 4. In the first, the solid line, the LSS torque is sampled at a rate of 500 Hz. As shown by these data, each tooth sees one major stress cycle and several smaller cycles per engagement. In the second set of time series data, the dashed line, the LSS torque is sampled at a rate equivalent to one sample per tooth engagement, i.e., at approximately 32 Hz. As one would expect, the relatively small stress cycles have disappeared and the magnitude of the stress cycle on each tooth may or may not be equal to maximum stress imposed on the tooth; e.g., see the load on tooth 4 in Figure 4b. As shown in this figure, the torque histogram for this turbine varies faster than the tooth engagement rate of 32 Hz; thus, data sample rates at the 32 Hz rate typically miss the highest loads on the teeth.

Rainflow Cycle Counts. One commonly used algorithm used to determination of the number of stress cycles contained



a. Low-Speed Shaft Torque



b. Torque on the Gear Teeth

Figure 4. Typical Time Series for the Low-Speed Shaft Torque on the Test Bed.

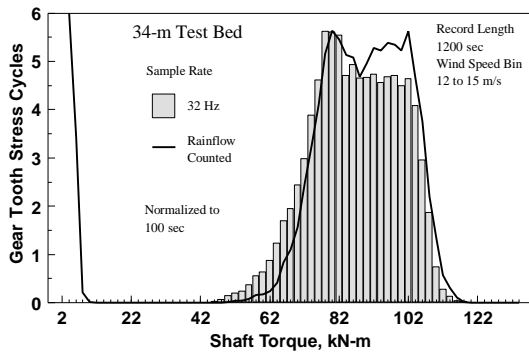
in a histogram of loads is the “rainflow counting algorithm” described by Downing and Socie (1982). This algorithm, as implemented by Sutherland and Schluter (1990) in LIFE2 fatigue analysis program for wind turbines, was used to count the cycles on the gear teeth of the Test Bed. In this analysis, two 600-second data sets, taken at 500 Hz sample rate (0.15 sec of these data are shown in Figure 4), were analyzed.

The initial step in the analysis is to process the LSS torque time history to obtain the tooth loads; namely, Figure 4a must be divided into the loads shown in Figure 4b. To analyze the loads on a single tooth, the LSS torque data are zeroed for all time that the tooth is not engaged. As this technique would

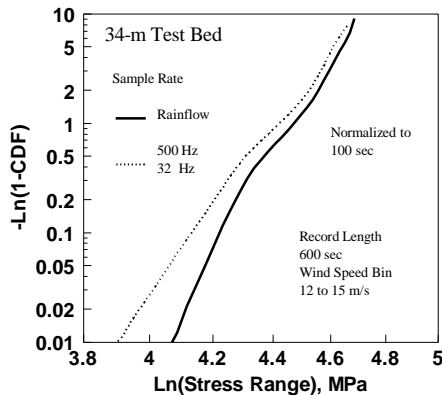
significantly reduce the data available for analysis, we examine the loads on an “average” tooth here. For this analysis, the LSS time history is modified by adding a zero value for each time a tooth engages or disengages, i.e., approximately every 0.3 seconds. The rainflow counter will then count the fatigue cycles on all of the gear teeth. And, the average fatigue load cycles are obtained by dividing the total by the number of teeth on the gear. This procedure is equivalent to computing the cycles of each tooth and then averaging the results.

The results of the rainflow analysis of the 500-Hz sample rate data are shown in Figure 5 as the solid line. As expected and shown in Figure 5a, each tooth is subjected to a large number of relatively low-magnitude cycles and one large cycle per engagement. The low-magnitude cycles are not included in Figure 5b.

When the same time history is analyzed at a slower sample rate, e.g., at one data point per engagement, the relatively small cycles disappear. And, because this relatively slow, fixed-interval data sampling rate will typically miss the highest stress in each tooth engagement, the relatively high stress cycles are shifted to lower stress values, as shown by the dashed line in Figure 4. The implication of this shift on service lifetime



a. Linear Histogram



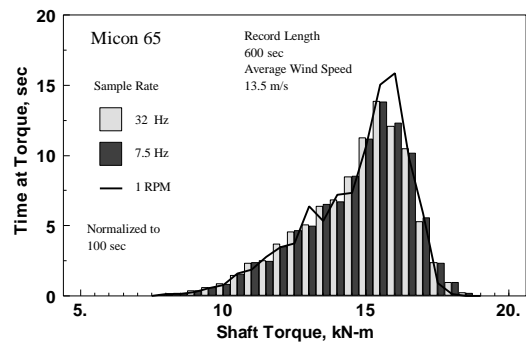
b. Weibull Plot

Figure 5. Stress Cycles on the Gear Teeth of the Test Bed.

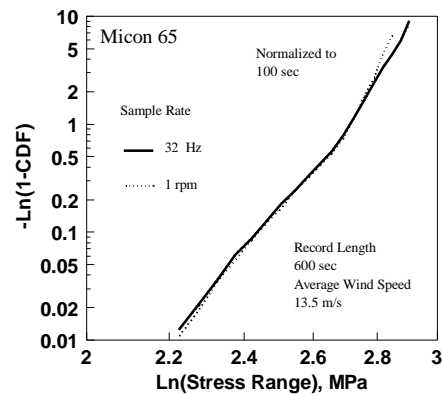
(damage) is discussed below.

Time-at-Torque. As discussed above, a macro-approach to the determination of the stress cycles is based on the time-at-level histogram of the torque, or, the time-at-torque histogram. In this analysis technique, the torque is assumed to be a slowly varying function of time. Thus, each tooth is subjected to a single cycle during each engagement. If the data rate for this analysis is equivalent to one sample per tooth engagement, then it yields exactly the same results as the rainflow counting technique for data sampled at the same rate.

Another form of this presentation is the time-at-torque histograms used by McNiff, Musial, and Errichello (1990). In this form, the torque histogram is binned by magnitude. The number of stress cycles on an average gear tooth is determined from this histogram by dividing the time in each torque bin by the duration of a tooth engagement (or, conversely, multiply by the rate of tooth engagement) and, then dividing by the number of teeth on the gear. Thus, the cycle count histograms and the time-at-torque histograms are simple multiples of one another. The time-at-torque histogram for the Micon 65 is shown in Figure 6.



a. Linear Histogram



b. Weibull Plot

Figure 6. Time-at-Torque Histogram for the Micon 65 .

Since the time-at-torque technique assumes that the torque is a slowly varying function of time, histograms taken at different data sample rates are comparable. As shown in Figure 6a, a significantly slower sample rate changes the distribution only slightly. For the Test Bed, data taken at a 500 Hz data rate and at 32 Hz are essentially the same, see Figures 5b and 7.

In addition to this point-by-point analysis, another common technique for determining the time-at-torque histogram is to bin the torque by its one-rotor-revolution average. The time series data for the Micon 65 and the Test Bed were also processed in this manner. As shown in Figures 6 and 7, the resulting distribution, labeled 1 rpm in the figures, is different from the other distributions.

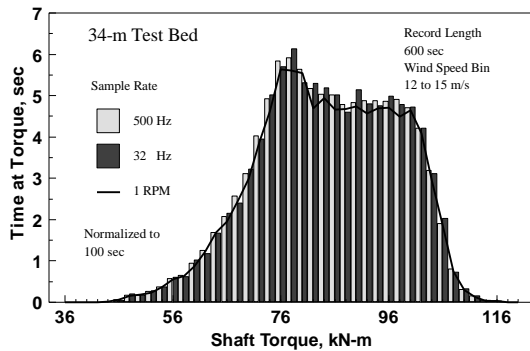


Figure 7. Time-at-Torque Histogram for the Test Bed.

DAMAGE CALCULATIONS

To ascertain the significance of the differences in the cycle count distributions cited above, the cumulative fatigue damage for an “average gear tooth” for each of the above distributions was determined. The analysis uses the techniques described in the AGMA Standard (1976); i.e., Miner’s Rule with the S-N diagram cited in Figure 1.

For the purposes of this paper, only one gear will be analyzed for each turbine. And, the analysis will be limited to bending fatigue of the gear teeth.

Micon 65. The analysis of the Micon 65 gearbox by McNiff, Musial, and Errichello (1990) indicates that the low-speed pinion gear has the shortest life. The tensile bending stress at the root fillet is related to shaft torque by a factor C_T . Namely,

$$\sigma_T = C_T \cdot S_T, \quad (1)$$

where σ_T is the bending stress and S_T is the shaft torque. They determined that C_T is equal to 16.095 MPa/kN-m.

As shown in Figure 6a, the largest torque in the LSS of the Micon 65 lies in the 18.5 to 19 kN-m bin. Thus, the maximum observed stress is approximately 306 MPa. As noted in Figure 1, this places all of the loads on the gear tooth below the fatigue

limit. Thus, this gear can operate almost indefinitely under these operating conditions. And, the differences between the 32 Hz, 7.5 Hz and 1 rpm distributions are not significant from a damage standpoint.

This result is consistent with McNiff, Musial, and Errichello (1990). They demonstrate that the gearbox failures for this turbine are caused by the high torque transmitted by the gearbox during braking.⁵

High-Torque Analysis for the Micon 65. While these results indicate that the Micon 65 gearbox has a conservative design for its operating loads, they do not provide an insight into the significance of the differences, from a damage standpoint, in the torque distributions at different sample rates. To better ascertain these differences, we will assume that C_T is equal to 160.95 kPa/kN-m, i.e., 10 times greater than is the actual case. As noted in Figure 1, this places all of the loads on the gear tooth above the fatigue limit.

The normalized cumulative damage diagram for this analysis is shown in Figure 8. In this figure, the damage has been normalized to the total damage as calculated from the 32-Hz data. As shown in this figure, the two torque distributions predict essentially the same damage, with the total damage within 4 percent of one another. The 32-Hz torque distribution predicts the highest damage (shortest service time).

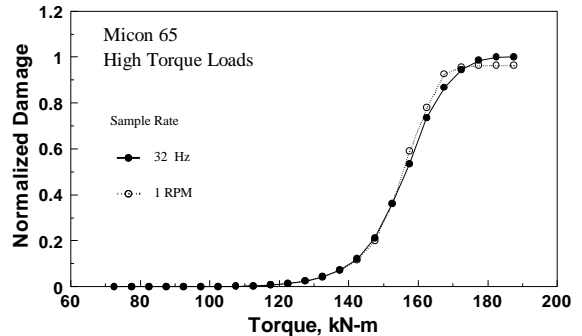


Figure 8. Accumulated Damage for the Pinion Gear on the Micon 65.

Test Bed. The damage analysis of the Test Bed gearbox also examines the stresses on the low-speed pinion gear. For this gear, the tensile bending stress at the root fillet is also related to shaft torque by the factor C_T , see Equation 1. For the analysis of this gearbox, C_T is divided into two factors; namely,

$$C_T = C_i \cdot C_d, \quad (2)$$

where C_i is the bending stress factor and C_d is the “derating” factor. C_i is equal to 1.18 MPa/kN-m for this gear. C_d typically

⁵The braking loads are not analyzed here because time series data for these events are not available.

ranges from 1.0 to 1.5 for an AGMA (1976, 1989) “quality number” of 10. For this analysis, we will take an intermediate value of 1.2. Thus, C_r equals 6.51 MPa/kN-m.

As shown in Figure 5, the largest torque in the LSS of the Test Bed lies in the 131 to 133 kN-m bin. Thus, the maximum observed stress is approximately 866 MPa. As noted in Figure 1, this places most of the loads on the gear tooth above the fatigue limit.

The normalized cumulative damage diagram is shown in Figure 9a for the 32-Hz data rate and for the rainflow counts. Figure 9b illustrates the 32-Hz and the 1-rpm data. In both plots, the damage has been normalized to the total damage as calculated from the rainflow counts bins.

As observed in Figure 9b, the damage predictions for the two macro (time-at-torque) samples indicate that the predicted service lifetimes are within a couple of percent of one another. The 1-rpm data predicts the highest damage (shortest lifetime).

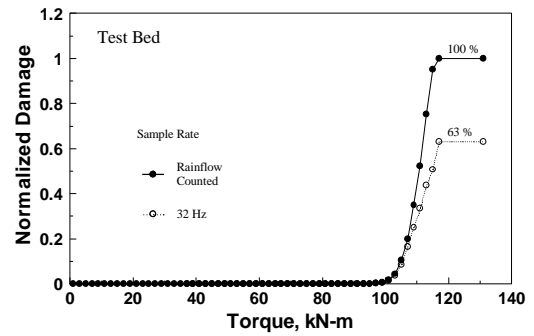
In Figure 5, the micro (rainflow) and the macro distributions do differ from one another. Damage calculations, see Figure 9a, illustrate that the damage predictions differ by approximately 37 percent, with the macro distribution predicting the longest lifetime (smallest damage) for the gearbox. It is a generally accepted truth that fatigue predictions within a factor of 2 are within the “noise” of prediction capability. Thus, the two distributions do not produce significantly different damage predictions.

Comparing Figures 5a and 9a, one notes that the large number of stress cycles below approximately 40 kN-m in Figure 5 all lie below the fatigue limit for the steel gear teeth. Thus, they do not contribute significantly to the fatigue damage of the gear teeth.

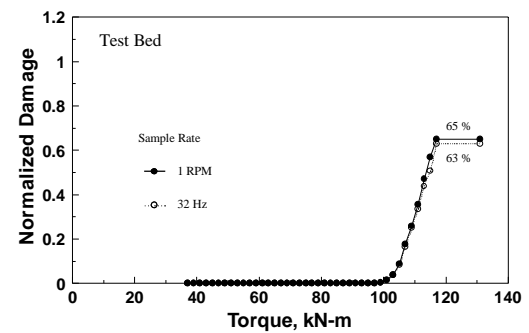
Fatigue Exponent. As was observed by Winterstein, see the discussion in Sutherland and Butterfield (1994), there is a direct link between material fatigue properties and the sensitivity of the predicted service lifetime (damage) to the tail of the load distribution tail. For materials with low-fatigue exponents (slope of the S-N curve), the accumulated damage is primarily derived from the body of the distribution. Thus, the damage accumulation in metal gears (they typically have low fatigue exponents) from the tail of the distribution is relatively small. Figures 8 and 9 support this trend.

SUMMARY

The time histories of the torque loads from two classes of wind turbine gearboxes, one a HAWT and the other a VAWT, are analyzed here to compare and contrast two techniques for characterizing the cyclic loads on the gear teeth. The first is a time-at-torque technique and the second is the rainflow-counting technique. As illustrated in the analyses, the two techniques yield different distributions for the stress cycles imposed upon the gear teeth. And, differences in the data sample rate also produce differences in the distributions. However, a damage analysis illustrates that these differences are minimal (a few



a. Rainflow Counted Data



b. Increased Sample Rate

Figure 9. Accumulated Damage for the Pinion Gear on the Test Bed.

percent to a maximum of 37 percent), from a damage standpoint, for the two turbines investigated here.

The analyses also offer additional insights into the characterization of the torque loads on the gearbox. First, the torque loads on the gearbox need to be examined with a relatively high sample rate data set. If the torque loads are a slowly varying function of time, then the differences in the time-at-torque and the rainflow distributions are not significant in terms of the damage predictions for the gear teeth. And, relatively slow and relatively fast data sample rates yield essentially the same damage predictions. For the turbines investigated here, the damage analyses do indicate that the time-at-torque technique based on a point-by-point data analysis yields essentially the same damage estimate as a time-averaged technique data analysis.

In both cases examined here, the torque loads were slowly varying functions of time. However, if the torque loads on the gearbox are not a slowly varying function of time, then a rainflow analysis may yield a significantly different distribution. In that case, gearboxes must be evaluated on an individual basis.

BIBLIOGRAPHY

Akins, R. E., 1990, "Cross-Spectral Measurements in the Testing of Wind Turbines," *Ninth ASME Wind Energy Symposium*, D. E. Berg (ed), SED-Vol. 9, ASME, pp. 155-161.

AGMA Standard, 1976, *Standard - Design Guide for Vehicle Spur and Helical Gears*, AGMA 170.01-1976, American Gear Manufacturers Association, Alexandria, VA.

AGMA Information Sheet, 1989, *Geometry Factors for Determining the Pitting Resistance and Bending Strength of Spur, Helical and Herringbone Gear Teeth*, AGMA 908-B89, American Gear Manufacturers Association, Alexandria, VA.

Downing, S. D., and Socie, D. F., 1982, "Simple Rainflow Counting Algorithms," *International Journal of Fatigue*, Vol. 4, No. 1, p. 31.

McNiff, B. P., Musial, W. D., and Errichello, R., 1990, "Variations in Gear Fatigue Life for Different Wind Turbine Braking Strategies," *Windpower '90*, p. 131.

Osgood, C. C., *Fatigue Design*, 2nd Edition, Pergamon.

Sutherland, H. J., and Butterfield, C. P., 1994, "A Summary of the Workshop on Fatigue Life Methodologies for Wind Turbines," *WindPower '94*, AWEA, Washington, DC.

Sutherland, H. J., and Schluter, L. L., 1990, "Fatigue Analysis of WECS Components Using a Rainflow Counting Algorithm," *Windpower '90*, AWEA, Washington, DC, pp. 85-92.

Veers, P. S., 1990, ed., *Selected Papers on Wind Energy Technology, January 1989-January 1990*, SAND90-1615, Sandia National Laboratories, Albuquerque, NM.